

# Influence of Processing Rate and Formulation on the Interface Strength of Vinyl Ester/E-Glass Composites

W. G. McDONOUGH<sup>1\*</sup>, J. P. DUNKERS<sup>1</sup>, G. A. HOLMES<sup>1</sup>,  
E. FERESENBET<sup>1</sup>, Y. H. KIM<sup>2</sup>, and R. S. PARNAS<sup>3</sup>

<sup>1</sup>National Institute of Standards and Technology, Gaithersburg MD 20899

<sup>2</sup>Korea Maritime University, Pusan, Republic of Korea

<sup>3</sup>University of Connecticut, Department of Chemical Engineering,  
Storrs, CT 06269

The single fiber fragmentation test was used to investigate the effect of gelation time on interfacial shear properties of fast reacting resin systems. We developed a processing system capable of producing single fiber fragmentation samples with gelation times that ranged from 2 min to 45 min. The interfacial properties of E-glass fibers in vinyl ester resin were measured with single fiber fragmentation tests using a manual and an automated testing machine. We found that vinyl ester resins catalyzed with methyl ethyl ketone peroxide and promoted with cobalt naphthenate and dimethylaniline gelled in less than two minutes and had an estimated interfacial shear strength of 105 MPa. Specimens cured without the promoter gelled in 45 min and had an interfacial shear strength of 72 MPa. Further curing of the unpromoted specimens resulted in an increase in shear strength to 96 MPa. We have demonstrated the ability to make and test rapidly cured specimens, thus expanding the range of materials that can be tested using the single fiber fragmentation testing technique.

## INTRODUCTION

An important issue for promoting the use of polymeric composites is a clearer understanding of the influence that processing conditions have on the final properties of fabricated parts. A composite system of particular interest to industries such as automotive and infrastructure is vinyl ester reinforced with glass fibers. One of the reasons for this interest is the flexibility that vinyl esters have in formulation and cure schedule such as: a short cycle time, rapid and controllable gel time, low viscosity for rapid wet-out and flow-through at high reinforcement levels, compatibility with the reinforcing material, good physical and thermal properties, and good fatigue performance (1).

Optimizing the processing of composites typically means trying to obtain the best trade-off between processing and properties to yield the most economical product. To this end, standards of measurement

are needed that can give us an unambiguous understanding of the changes that can occur in the final properties as we change the processing conditions. One important area where we need to measure these changes is in the interfacial phase that develops from the interaction of the fiber with the polymer matrix, since this phase exerts a profound influence on the final properties of the composites. This influence is due to the extensive internal surface area that the interface occupies in the composite microstructure, which can be as high as 3000 cm<sup>2</sup>/cm<sup>3</sup> (2). Because the interfacial region plays such an important role in determining mechanical properties and long-term durability of composites, there is a need for appropriate methods to assess changes in the strength and stability of the interface. Traditionally, fracture techniques such as short beam shear tests have been used to study composite interfaces. However, interpretation of the failure mechanisms from these bulk property tests can be difficult because of the interaction of many competing failure modes that accompany composite fracture. By contrast, micro-mechanical test techniques such as the single fiber fragmentation test (SFFT) have the potential to reduce the complexity of events that confound interfacial failure analysis.

\*To whom correspondence should be addressed.

National Institute of Standards and Technology, Polymers Division, 100 Bureau Drive, Stop 8543; Gaithersburg, MD 20899; walter.mcdonough@nist.gov.

In the single fiber fragmentation test, a dogbone specimen is made with a resin having a single fiber embedded down the central axis. The sample is pulled in tension and stress is transmitted into the fiber through the fiber-matrix interface. Eventually, the fiber breaks at its weakest flaw as the strain is increased. The fragmentation process can continue upon further loading because of the interaction between the fiber and matrix at the interface. This process of fiber breakage continues until the remaining fiber fragments are all less than a critical transfer length ( $l_c$ ). At this point, the fragmentation process has reached saturation. Once saturation has been reached, the specimen is allowed to relax back to the unstressed state, the fragment lengths are measured, and then a micro-mechanics model is used to estimate the interfacial shear strength.

Typically, the Kelly-Tyson Model (3), where the matrix is assumed to be elastic-perfectly plastic, is used to calculate the interface strength. Another method that has been used is the Cox Model (4), wherein the matrix is assumed to be linear elastic.

Fragmentation of E-glass fibers during interfacial adhesion tests of an epoxy SFFT specimen have been shown by Holmes *et al.* (5) to occur when the matrix is exhibiting nonlinear viscoelastic behavior. In addition, previous work in this laboratory has shown that polyisocyanurate SFFT specimens also exhibited nonlinear viscoelastic behavior during fiber fragmentation (6). Hence, a nonlinear analytical procedure was deemed necessary to more accurately assess the interfacial shear strength at the fiber matrix interface. This analytical procedure is based on the non-linear viscoelastic model developed by Holmes *et al.* to account for the time dependent and non-linear viscoelastic effects of the matrix during the single fiber fragmentation test. This accounting was done by replacing the Young's modulus used in the Cox equation with the time and strain rate dependent secant modulus. One conclusion of the research by Holmes was that the Kelly-Tyson model underpredicted the interfacial shear strength that is observed and the Cox model overpredicted the interfacial strength that is observed.

For the research presented in this paper, we chose a vinyl ester resin that permitted a wide range of processing conditions. The vinyl ester resin system reacts with styrene to form a cross-linked structure through addition polymerization promoted by peroxide catalysts.

Ziaee and Palmese (7) have investigated the relationships among cure temperature, chemical kinetics, microstructure, and mechanical performance for the vinyl ester resin systems. They cured a Dow Derakane 411-C50 resin system at 30°C and 90°C, and postcured these systems at 125°C. They found that the initial cure temperature significantly affects the mechanical behavior of the system examined. The tensile strength and fracture toughness of systems cured at 30°C followed by the postcure at 125°C were significantly higher than for those specimens cured at 90°C

and postcured at 125°C. They found that the ratio of vinyl ester to styrene double bonds incorporated into the network was greater for the 30°C cure than for the 90°C cure. In related research, Dua *et al.* (8) studied the copolymerization kinetics of styrene/vinyl ester systems and found that the cure behavior of vinyl ester resins is affected not only by the chemical reactivity of the monomers towards the free radicals, but also by diffusion effects, phase separation, and microgel formation. Some of their other conclusions were that during the initial stages of cure, the rate of conversion of styrene monomer is lower than that of vinyl ester double bonds, but that during the latter stages of cure, the styrene continues to react well after the vinyl ester reaction has ceased.

For this paper, we used the single fiber fragmentation test to assess the effect that processing has on the interfacial properties of vinyl ester/E-glass composites. More importantly, we wanted to expand the use of the single fiber fragmentation test to include rapidly cured composite systems.

## MATERIALS

The resin system used was a vinyl ester resin containing a mass fraction of 0.45 styrene (Derakane 411-C50 Dow Chemical Company). Polymerization was carried out using various formulations containing methyl ethyl ketone peroxide (MEKP, Aldrich Chemical Company) as the catalyst, and dimethylaniline (Aldrich Chemical Company) and cobalt naphthenate (CMG Americas Inc.) as a promoter package. The fibers used were E-glass fibers (Owens-Corning Fiberglas) with a proprietary size.

## Mold Preparation

Typically, samples made for testing in the single fiber fragmentation machine have been cast in open faced molds (9). Although this process works well for resin systems containing components with low volatility, we found the volatility of the styrene in the vinyl ester to be too high to cast specimens in open molds reproducibly. In addition to the loss of styrene monomer, we observed significant shrinkage in the open faced cured specimens. To solve this problem, we chose to modify an existing mold used for resin transfer molding (10, 11). A ten-cavity aluminum insert was placed inside the main spacer plate (see *Fig. 1*).

Single filaments were placed in the mold template and centrally aligned through the notches in the sprue zones. The fibers were attached by using drops of an epoxy resin (Hardman Adhesives). DuPont Kapton film was taped to the spacer plates and was also coated with mold release agent. These films were added to help in the removal of the cured specimens from the cavity and to impart a smooth surface finish so that further polishing would not be needed. Between the top and bottom platens and the respective spacer plates, we placed sheets of a compressible rubber mat (Potomac Rubber). After the mold insert

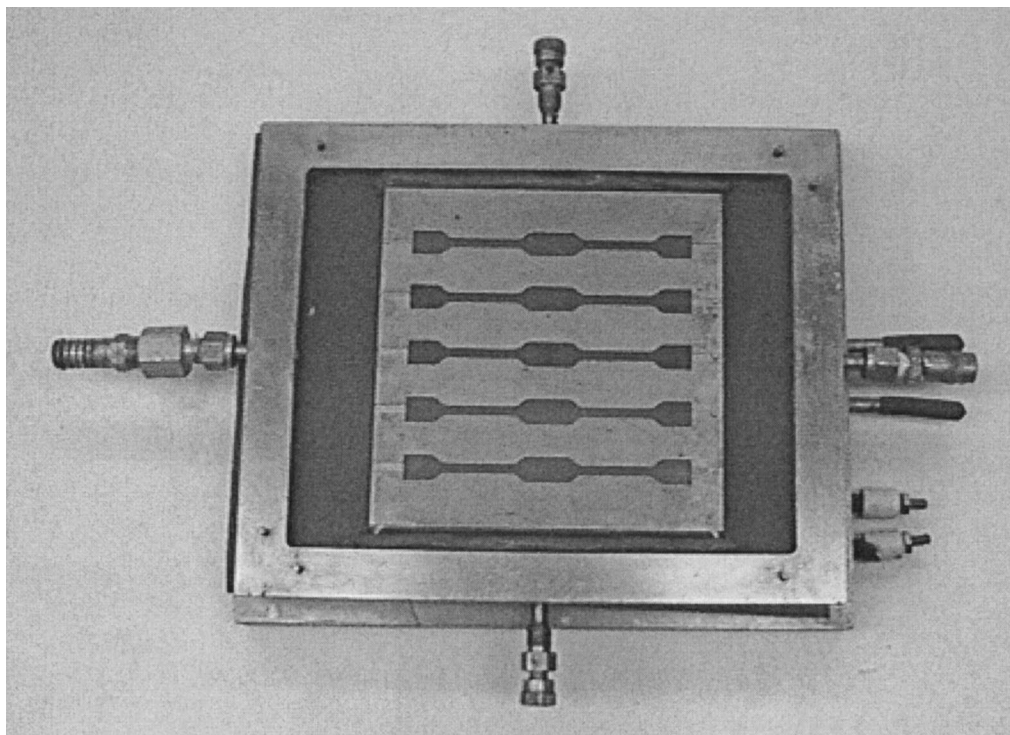


Fig. 1. Molding apparatus used in this study. Single filaments are placed in the dogbone cavities, and after the mold is closed, resin is injected from left to right.

and spacer plates were stacked into the mold cavity, we put tacky tape into the channels on both sides of the inserts. This tape, combined with the compressible rubber sheets, forced the injected resin to flow through the sprue openings and into the cavities containing the fibers. Before the mold was placed in the press (Wabash Metal Products, Inc.), a thick-walled rubber hose was attached to the outlet port of the mold assembly. The other end of the outlet hose was attached to a pressure source that would eventually supply back pressure to the mold. We also attached a thick-walled hose to the inlet port. The press was closed to apply enough pressure to the mold to prevent leakage when the resin was injected. The mold was then heated to 80°C and allowed to equilibrate for 1 h.

### Molding Procedure

We were interested in assessing the relationship between the time to gelation and the interfacial shear properties. We chose MEKP as our catalyst and varied the amount mixed with the vinyl ester to obtain gel times that were far enough apart to see measurable differences in mechanical properties. We found that when a mass fraction of 0.02 MEKP catalyst was added, we achieved a gel time of approximately 40 min at 80°C (cured at 80°C for 1 h and then cured at 90°C for 2 h) (procedure A). We also repeated procedure A and extended the curing time at 90°C from the 2 h for Procedure A to 7 h in an effort to increase the

glass transition temperature ( $T_g$ ) (procedure B). When we added a mass fraction of 0.10 MEKP, we achieved a gel time of approximately 10 min (cure cycle of 25 min at 80°C and 2 h at 89°C) (Procedure C). We also wanted to achieve a gel time of less than 2 min, but this goal could not be achieved by simply adding more catalyst. We found that if we added a mass fraction of 0.02 MEKP with a mass fraction of 0.002 dimethylaniline together with a mass fraction of 0.001 cobalt naphthenate as the promoter package, we achieved a gel time of 2 min (cure cycle of 17 min at 80°C followed by 2 h at 90°C) (Procedure D). These gel times were measured by placing resin into test tubes, placing the tubes into an oven set at 80°C, and determining when gelation occurred by visual inspection through the use of a probe. The difference in heat transfer rates between the test tube observations and the sample molding procedure is expected to produce shorter gelation times in the molded samples, and should be especially important in the fastest reacting system used in Procedure D.

For each of the systems examined, the mixing and molding procedures were similar. The catalyst (and promoter package used in procedure D) were mixed and then degassed. We determined that 30 min were needed to guarantee void free specimens. Afterwards, we poured the resin into tubes that were then attached to an injection gun (Ellsworth Adhesive Systems) and connected the gun to the tubing that had been attached to the inlet port. Subsequently, we injected the resin into the mold cavity. When the resin

filled the mold cavity, we applied back pressure (103 kPa over atmospheric pressure). We then kept the mold at 80°C for a dwell time of the anticipated gel time plus an additional 15 min. Subsequently, we ramped the temperature to 90°C and then held the pressure for 2 h (7 h for procedure B). Afterwards, we turned off the heat and back pressure and allowed the mold to cool to room temperature slowly. The mold was then opened and the samples removed.

### Testing

After processing, the specimens were examined and any specimens that contained fibers that were wavy or broken were discarded. Two marks were placed on the specimen surface approximately 1 cm apart and perpendicular to the long axis of the specimen. These marks were used subsequently to measure the strain in the specimen during the test. After this preparation, the dimensions of the specimen (width and thickness) were measured using an electronic digital caliper (Fowler Max-Cal). The standard uncertainty in these measurements is 10  $\mu\text{m}$ . Finally, it should be noted that this process is a significant improvement over the open face molding in that the parts had very uniform dimensions (low uncertainty and variations) and were optically clear enough so that polishing was not needed.

Most of the single fiber fragmentation tests were carried out on a hand operated testing apparatus similar to the one described by Drzal and Herrera-Franco (9), and the details of the experiments can be found in Holmes *et al.* (12). During the test, a small step strain was applied manually by turning a knob attached to the movable grip of the apparatus. The strain increments are of the order of 0.1% strain. After the strain increment, there was a delay of 10 min before the next step-strain. We determined that the fragmentation process depends on the viscoelastic properties of the matrix, and that 10 min allows sufficient time for nearly all of the fragmentation to occur. At the 8 min point of each strain increment, the number of fragments and the strain were recorded. We needed to start counting the fragments at the 8 min point so that the count would be completed before the next strain increment was scheduled to start at the 10 min point. At saturation, the fragment lengths were measured. After each test was completed, the specimens were unloaded slowly and allowed to relax to an equilibrium length under zero stress, usually over the course of several hours, and the fragment lengths were again measured. The zero stress data were used to calculate the interfacial shear strength values. Residual strains were calculated from the differences in the length between the strain marks after testing to the length between the strain marks before testing. For this work, the value of the fiber modulus was taken from Schultheisz *et al.* (13) as 67.5 GPa and the value for the Poisson's ratio for the matrix was taken from Whitney *et al.* (14) as 0.35.

In addition to using the manual single fiber fragmentation testing machine, we also used an automated single fiber fragmentation machine (TRI Princeton, N.J.) (Fig. 2). The automated machine provides a level of loading repeatability that cannot be matched manually. Because of strain to failure issues with specimens made using Procedure B, we found it necessary to use the automated machine. With the automated machine, an image of the fiber is scanned after each loading step. These images are then archived for subsequent analysis. In a manual test, visual information that exists at each loading step is lost when the load is changed. On the automated fragmentation machine, we preprogram the strain rates, strain increments, and delay times after each loading step.

We then scan the length of the sample and bring the fiber into focus. Subsequently, we start the loading routine, and, aside from occasionally refocusing the camera on the fiber, the test proceeds automatically. After the test is completed, we save the scanned images to a writeable CD-disk and analyze the images off-line. In addition to the images, the load vs. time data has also been saved. From these images, we then measure the fragment lengths at each strain step. Some of the advantages of the automated machine over the manual machine are repeatability of loading, better precision of the measurements, time and labor savings to the operator, and data archiving. Data archiving is a very powerful benefit, because it is now possible to send the images to researchers who are developing more complex analytical methods to measure the interfacial shear properties. The uncertainties for the automated machine are comparable to the manual machine.

### Near Infrared Spectroscopy

Fourier transform near infrared spectra were used for calculating conversion and were collected from 7900  $\text{cm}^{-1}$  to 4000  $\text{cm}^{-1}$  using a Nicolet Magna 550 bench equipped with a white light source, calcium fluoride beamsplitter, and indium antimonide detector. Transmission spectra were collected on the SFFT specimens using 16 scans with a 4  $\text{cm}^{-1}$  resolution, referenced to air. Pure vinyl ester and pure styrene were used as received from Dow and CMG Industries, Inc., respectively, for calibration purposes.

A 6300  $\text{cm}^{-1}$  to 5600  $\text{cm}^{-1}$  region of the spectrum was analyzed to determine the consumption of the vinyl groups belonging to the vinyl ester (VE) and the styrene (STY). Peaks attributed to the vinyl ester group and styrene group in the Derakane 411-50 were determined by analyzing separate spectra of VE and STY. The internal standard (STD) peak used for these calculations is a carbon-hydrogen stretch overtone present at 5667  $\text{cm}^{-1}$ . Additional confirmation of peak assignments is provided in the literature.

The PeakFit program (Jandel) was used to baseline correct and fit peaks to the region of interest of the absorbance spectra. Peak fitting provides a measure

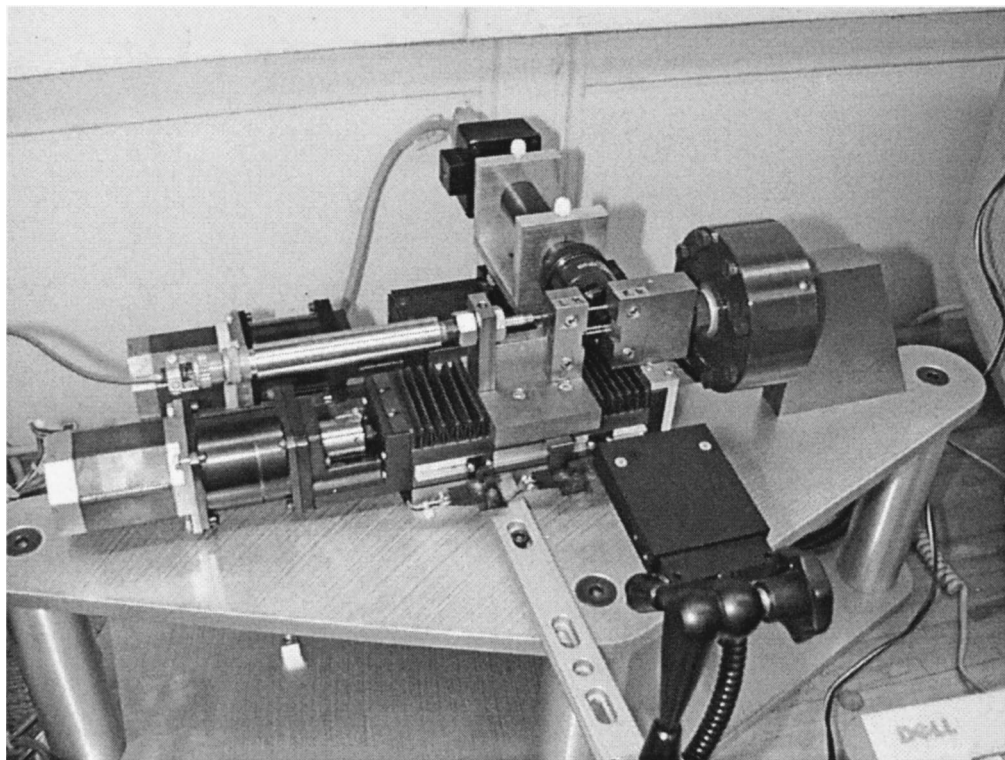


Fig. 2. Automated single fiber fragmentation machine.

of area occupied by a peak that in turn reflects the concentration of species present. To calculate remaining species, the area attributed to either the VE or the STY was then divided by the area of the STD of each SFFT specimen. This ratio was then normalized to the corresponding VE/STD or STY/STD for the unreacted Derakane 411-50 resin to obtain the fractional remaining species. The converted species were calculated by:  $100\% \times (1 - \text{remaining species})$ . The absorbance standard uncertainty was taken as the root-mean-square of the variation in the baseline absorbance value from  $9600 \text{ cm}^{-1}$  to  $9400 \text{ cm}^{-1}$  and has a value of 0.0003 absorbance units.

### Differential Scanning Calorimetry

The glass transition temperatures ( $T_g$ s) were estimated using a differential scanning calorimeter (DSC) (Perkin-Elmer DSC-7) with software provided by the manufacturer. Specimens were scanned at  $10^\circ\text{C}$  per min from  $40^\circ\text{C}$  to  $160^\circ\text{C}$ .

## RESULTS AND DISCUSSION

### Processing

Two important processing issues required attention: 1) molding void-free vinyl ester/E-glass fiber SFFT specimens, and 2) controlling the cure so the specimens had an acceptable strain to failure. For the first issue, when we prepared the formulations used for procedures A to C, we noted that stirring entrained air and significant time was needed for the resin to degas.

To minimize styrene loss, we did not pull a vacuum on the system. When we made specimens following procedure D, we generated foam. Herzog *et al.* (15) noted that when vinyl ester resins are promoted with cobalt and catalyzed with methyl ethyl ketone peroxide (MEKP), gas is generated and this gas has been a problem with vinyl ester users for many years. Commercial MEKP's contain a small amount of hydrogen peroxide that remains as a reaction residual. The hydrogen peroxide rapidly decomposes in the presence of a non-shielded cobaltous complex with molecular oxygen evolving during the reaction, thus causing foaming that lasts 3 min to 5 min. They recommended waiting at least 5 min to 10 min after catalyzation to significantly lower the risk of encapsulating any foam. We also observed foaming in the formulations that contained cobalt naphthenate and MEKP during mixing. However, we found that we needed approximately 30 min for the bubbles to dissipate to the point where they were no longer observed in the molded test samples. Even with back pressure, we found that if we did not allow enough time for the foam to dissipate before we injected the resin, the samples contained porosity that led to stress concentrations. We used a 30 min delay before injecting the resins for all of the procedures, thus addressing the first processing issue. The cure cycles were chosen to solve the second issue. Curing at temperatures greater than  $90^\circ\text{C}$  resulted in samples too brittle to finish the fragmentation process in the fiber. Undercuring the samples resulted in matrix yielding before the end of the fragmentation

process. Thus, although the materials used for this work are used commercially, the cure cycles were chosen to give an acceptable strain to failure to use the single fiber fragmentation test and to choose processing conditions that resulted in differences in interfacial properties.

Figure 3 shows the near infrared (NIR) spectra of the unreacted Derakane 411-C50 and the spectra of its components, the pure vinyl ester and styrene. From this figure, it is evident that the shoulder on the Derakane spectra around  $6164\text{ cm}^{-1}$  originates from the carbon-hydrogen stretching overtone of the terminal vinyl group from the vinyl ester resin. The peak at  $6135\text{ cm}^{-1}$  is assigned to the vinyl group from the styrene. The internal standard band at  $5660\text{ cm}^{-1}$  is an aliphatic carbon-hydrogen stretching overtone. This peak was chosen because of its terminal position in the spectra which provides more consistent results than interior peaks.

Figure 4 shows the spectrum of unreacted Derakane 411-C50 resin along with the spectra from two dog-bone specimens. In this figure, small but discernable differences can be seen between the vinyl overtone regions of the 2 h (Procedure A) and 7 h (Procedure B) postcured samples. It is clear that upon curing, both peaks decrease in intensity and shift to lower wavenumbers. For the 2 h postcure, the vinyl ester and styrene peaks can be found at  $6147\text{ cm}^{-1}$  and  $6119\text{ cm}^{-1}$ , respectively. The vinyl ester band does not shift appreciably during the 7 h postcure while the styrene peak undergoes a  $6\text{ cm}^{-1}$  shift to  $6113\text{ cm}^{-1}$ .

The conversions of vinyl ester (VE), styrene (STY), and both vinyl ester and styrene together (VE + STY)

are presented in Fig. 5 for various processing conditions. Note that fewer than three spectra were used in the calculation of conversion for processing condition D, therefore no error bars were provided for this condition. For specimens made following procedures A and C, the VE reacted more than the STY. For specimens made following procedure B, the conversion of VE increased when compared to the 2 h postcure. The STY did not cure appreciably, resulting in a small increase in the total conversion of vinyl groups. For the specimens made following procedure C, the STY were more reacted than the STY groups from procedures A and B, which led to an overall higher conversion of vinyl groups. When the promoter was added (procedure D), the STY groups underwent more reaction than the VE groups. The total reaction of vinyl groups for the system with promoter was about 5% higher than for the specimens made following procedures A and B.

The  $T_g$ s for the specimens made by procedures A, B, C, and D were  $85^\circ\text{C}$ ,  $92^\circ\text{C}$ ,  $55^\circ\text{C}$ , and  $99^\circ\text{C}$  respectively, with a standard uncertainty of  $2^\circ\text{C}$ . Table 1 shows some of the cured properties of the systems examined in this paper. As can be seen, the 2% catalyst specimens cured with promoter (procedure D) provided a very strong, tough matrix. The 2% and 10% unpromoted specimens that had a 2 h postcure (procedures A and C, respectively) were very ductile and had residual strains of approximately 3%. The properties of the 2% catalyst specimens without the promoters eventually approached those of the promoted specimens when they were given a longer postcure (procedure B). More work needs to be done in

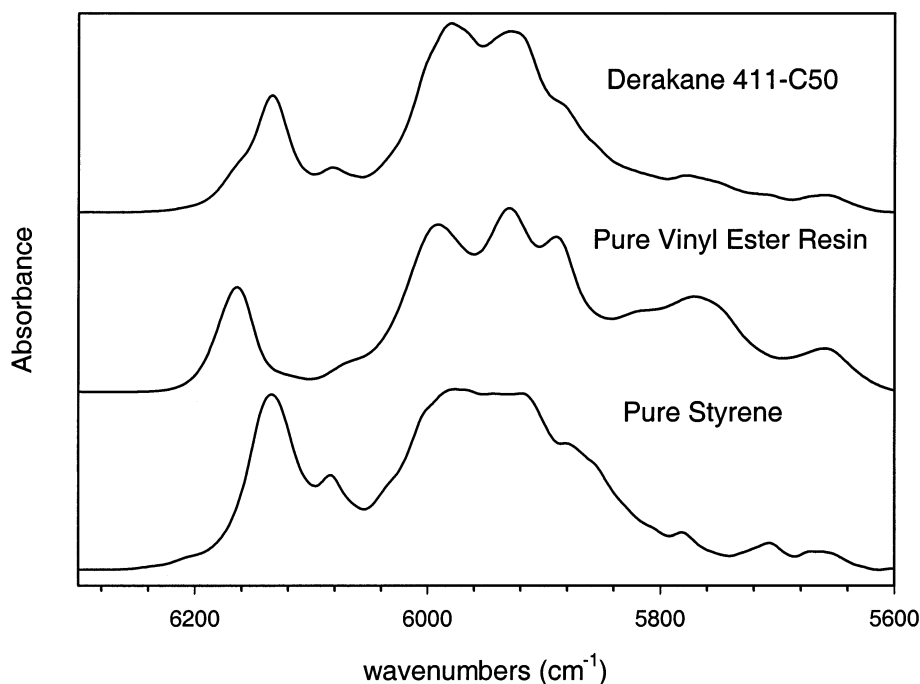


Fig. 3. Near IR spectra of the unreacted Derakane 411-C50, and the spectra of its components.

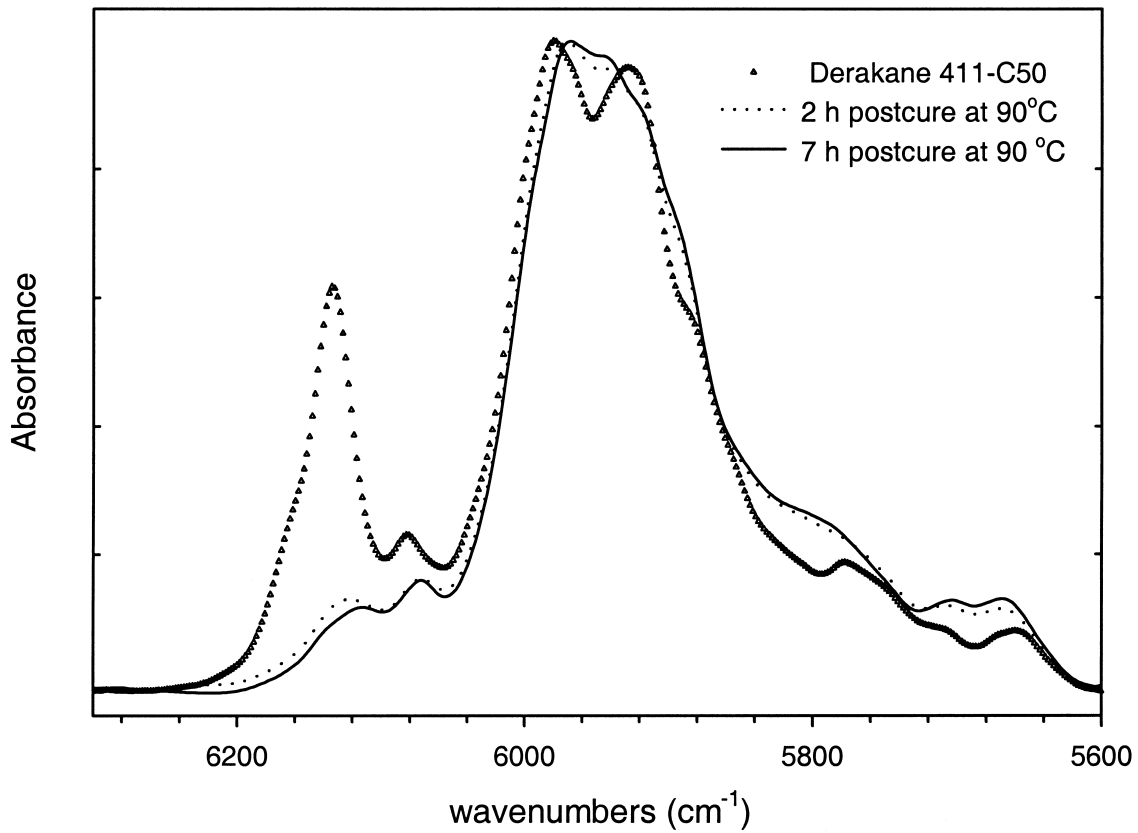


Fig. 4. Near IR spectra of the unreacted Derakane 411-C50 resin along with the spectra of two dogbone specimens. The specimens are both unpromoted systems with different postcure times (Procedures A and B).

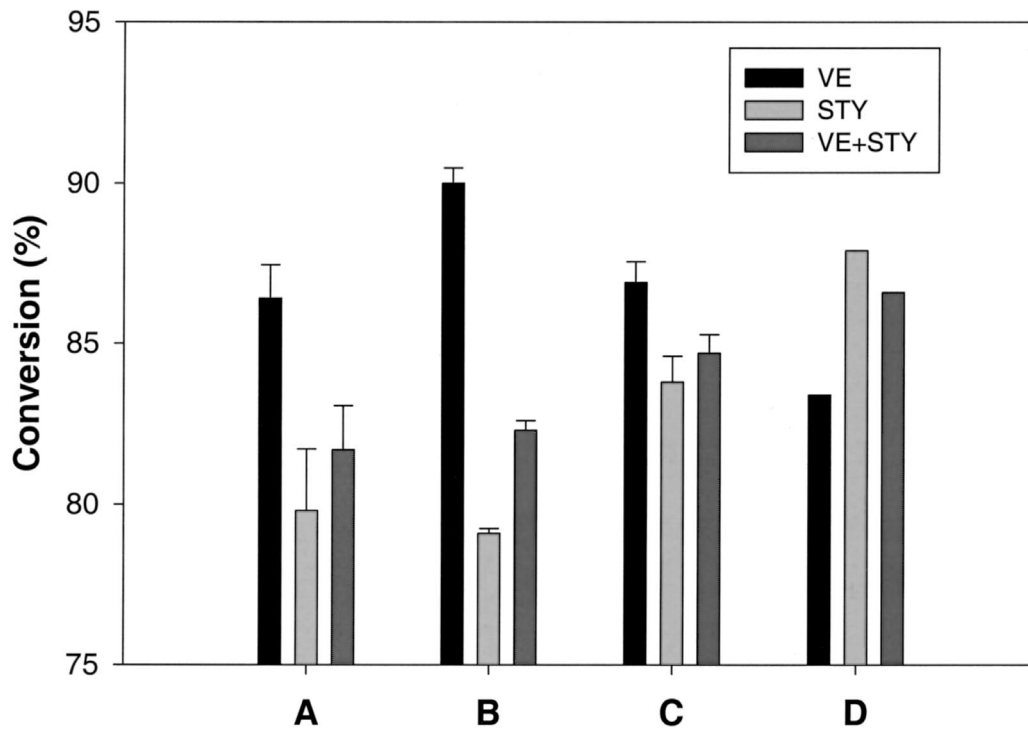


Fig. 5. Conversion of vinyl ester, styrene, and total vinyl groups for the four different resin formulations and processing schedules, A, B, C, and D.

Table 1. Processing Properties and Testing Results.

| Procedure* | Gel Time, min | Promoter | T <sub>g</sub> , °C | E <sub>matrix</sub> , GPa | Residual Strain | l <sub>c</sub> , μm | τ (Kelly-Tyson), MPa | τ (Holmes), MPa |
|------------|---------------|----------|---------------------|---------------------------|-----------------|---------------------|----------------------|-----------------|
| A          | 45            | No       | 85                  | 1.9                       | 3.0             | 845                 | 25.7                 | 72.4            |
| B          | 45            | No       | 92                  | 3.1                       | 0.2             | 674                 | 32.3                 | 96.0            |
| C          | 8             | No       | 55                  | 1.4                       | 3.0             | 1084                | 17.3                 | 44.3            |
| D          | 2             | Yes      | 99                  | 2.9                       | 0.2             | 607                 | 33.1                 | 104.6           |

\*Note: Curing cycles for the procedures were: (gel time + 15 min at 80°C followed by 2 h at 90°C. Procedure B called for 7 h at 90°C). τ is the interfacial shear strength as calculated either using the Kelly-Tyson model or the non-linear viscoelastic model developed by Holmes.

examining the chemical nature of the unpromoted and promoted systems to determine the level of chemical similarity. If the materials have significantly different chemical structures, then there may be long term and durability consequences that would need to be examined. For example, the NIR results do not fully explain the very low T<sub>g</sub> value obtained with curing Procedure C.

### Single Fiber Fragmentation Test

For this paper, we tested two specimens for the procedures, and we performed full mechanical analyses for one specimen at each condition. Such small numbers of specimens tested prevent us from being able to make statistically significant conclusions, however, the results will show that the range of materials that can be evaluated using the single fiber fragmentation test can be expanded to include fast reacting resin systems. We can see from the results of the fragmentation test in Table 1 that specimens made following procedures B and D had the highest modulus values (E<sub>m</sub>) and the lowest values for residual strain. Residual strain was calculated by comparing the length between the two strain markers that were placed on the specimens before and after they were tested. The stiffer matrices can be expected to transfer more stress into the fibers and, consequently, have more fragments at the end of the test. The number of fragments at saturation is reflected in the value for the average critical length, l<sub>c</sub>, and thus, in the estimated value for the strength of the fiber at the critical length. If we use the Kelly-Tyson equation, specimens made following procedures D and B had the highest values for the interface strength (τ) of 33.0 MPa and 32.3 MPa respectively. Specimens made using procedure A had a value of 25.7 MPa and specimens made with procedure C had a value of 17.3 MPa. If we look at the values that were calculated using the non-linear viscoelastic model, although the rankings are the same, the spacing between them is much greater. Procedure D yielded a value of 104.6 MPa, procedure B yielded a value of 96.0 MPa, procedure A yielded a value of 72.4 MPa, and procedure C yielded a value of 44.3 MPa. It is interesting to note that the interfacial strength values calculated by using the non-linear viscoelastic model gave results that were more indicative of how

the materials responded as seen in the stress-strain curve (Fig. 6). Specimens made following procedures A and C, both unpromoted 2 h post-cured resin systems, had similar stress-strain curves, and both had fairly large permanent sets of 3% residual strain. By contrast, specimens made following procedures D and B had a residual strain of approximately 0.2%, which was similar to the behavior of epoxy and polyisocyanurate specimens tested in this lab (5, 6).

In Fig. 6, note that the data from the specimen made following Procedure B has more data points than do the other specimens shown. It turns out that the automated machine does a better job at keeping a consistent strain increment. The manual machine tended towards higher strain amounts at each strain increment. Thus, when using a manual machine, the operator needs to determine the amount of strain that is actually applied to the specimen and make the appropriate adjustment for subsequent loadings.

### Interface Damage Zones

An interesting aspect of the failure or fragmentation process was the damage zones around the breaks in the fiber. In glass fiber epoxy matrix systems and glass fiber polyisocyanurate fragmentation samples, when breaks occurred they had small damage or debond zones, and these zones either remained along the interface or extended into the matrix (see Fig. 7). With the vinyl ester samples used in this study, we saw larger debond regions, which indicated a poorer interface bond. What was of particular interest, however, was the appearance of large discolored regions in the matrix upon relaxation to zero stress. Although such behavior may not be surprising in the specimens made following procedures A and C since the matrices in these specimens were very ductile and had significant permanent deformations, it was somewhat surprising to see it occur in the promoted system (procedure D) since the matrix in this system behaved more like an epoxy or polyisocyanurate. We have indications that the effect is independent of the commercial size that was on the fibers since similar testing has been done on fibers with a vinyl ester compatible silane and with unsilanized fibers using the same matrix, and we have observed these extended damage zones.

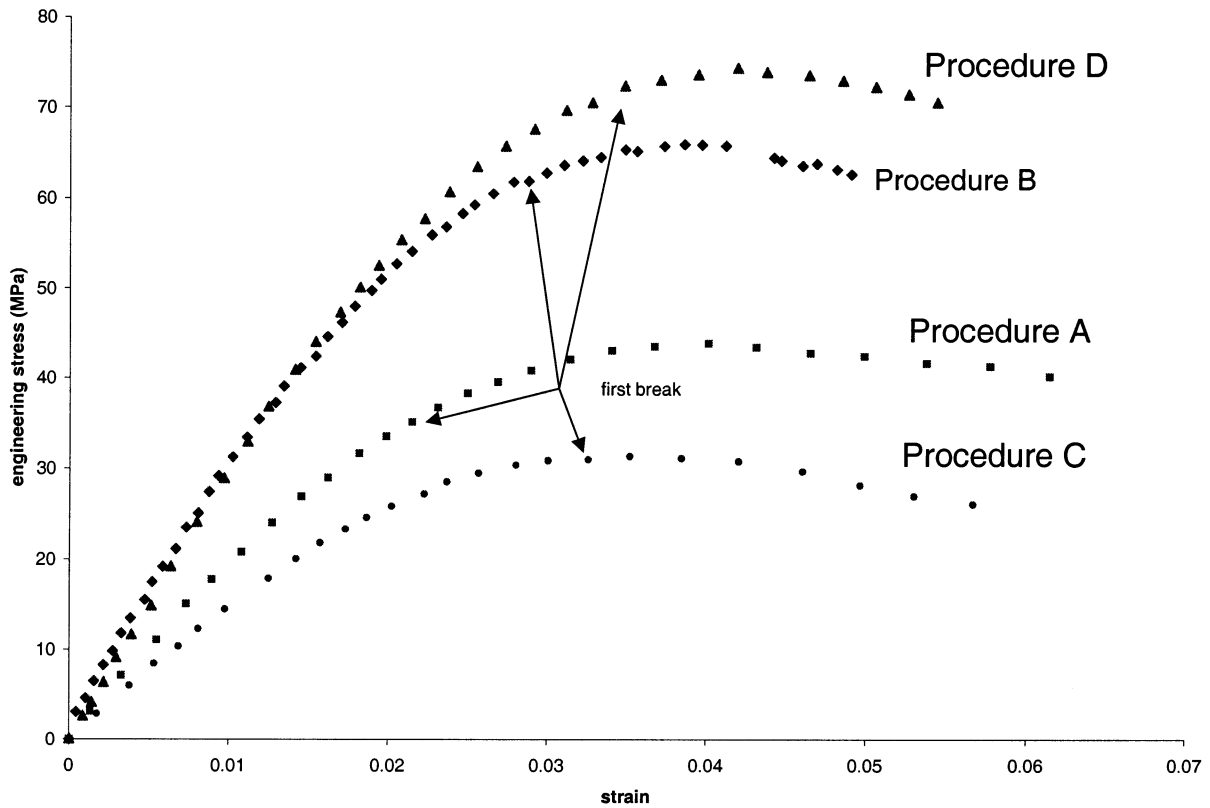
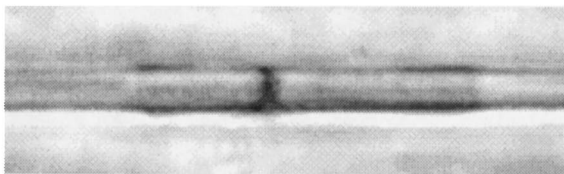
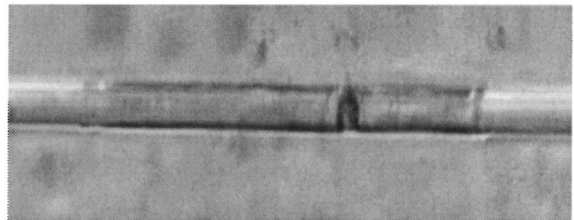


Fig. 6. Stress-strain curves for specimens made following the four different procedures, A, B, C, and D.

2-minute gel material also shows interfacial damage near fiber breaks



8-minute gel material shows extensive interfacial damage near fiber breaks



45-minute gel material also shows interfacial damage near fiber breaks



Classic epoxy system shows no interfacial damage near fiber breaks

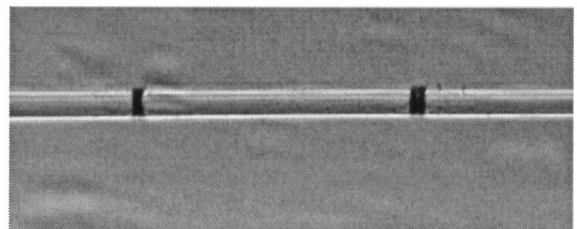


Fig. 7. Comparison showing how the damage regions of the vinyl ester specimens differ from epoxy resin fragmentation specimens. The damage zones appeared after the load was removed from the specimens.

## CONCLUSIONS

The processing technique described in this paper is a significant improvement over the open face molding in that the parts had very uniform dimensions (low uncertainty and variations) and were optically clear enough so that polishing was not needed. The range of materials that can be investigated using the single fiber fragmentation test has been expanded to include rapidly cured composite systems. In this work, we found that vinyl ester resins catalyzed with methyl ethyl ketone peroxide and promoted with cobalt naphthenate and dimethylaniline gelled in under two minutes and had an estimated interfacial shear strength of 105 MPa. Specimens cured without the promoter gelled in 45 min and had an interfacial shear strength of 72 MPa. Further postcuring of the unpromoted specimens resulted in an increase in shear strength to 96 MPa. The increase in postcuring time for the unpromoted system resulted in similar stress strain curves in the promoted specimens. More work needs to be done in examining the chemical structure of the unpromoted and promoted systems to determine the level of chemical similarity. If the materials have significantly different chemical structures, then there may be long term and durability consequences that would need to be examined. Finally, the authors note that, due to the small number of specimens tested, statistically significant conclusions cannot be made at this time.

## ABBREVIATIONS AND NOTATION

|        |  |
|--------|--|
| DSC    | differential scanning calorimeter                      |
| MEKP   | methyl ethyl ketone peroxide                           |
| NIR    | near infrared  |
| SFFT   | single fiber fragmentation test                        |
| STD    | infrared internal standard                             |
| STY    | styrene  |
| VE     | vinyl ester  |
| $T_g$  | glass transition temperature                           |
| $\tau$ | denotes the interfacial shear strength                 |
| $E_m$  | denotes the matrix modulus                             |
| $l_c$  | denotes the critical length of the fiber at saturation |

## REFERENCES

1. D. A. Babbington, J. M. Cox, and J. H. Enos, *Proceedings of the Third Annual Conference on Advanced Composites*, ASM International, 155 (1987).
2. K. K. Chawla, *Composite Materials Science and Engineering*, Springer-Verlag, New York, 81 (1987).
3. A. Kelly and W. Tyson, *J. Mech. Phys. Solids*, **13**, 329, (1965).
4. H. L. Cox, *British Journal of Applied Physics*, **3**, 72 (1952).
5. G. A. Holmes, R. C. Peterson, D. L. Hunston, and W. G. McDonough, *21st Annual Meeting of the Adhesion Society*, 175 (1998).
6. W. McDonough, G. Holmes, and R. Peterson, *Proceedings of the 13th Annual Technical Conference on Composite Materials*, American Society for Composites, 1688 (1998).
7. S. Ziaee and G. R. Palmese, *Journal of Polymer Science: Part B: Polymer Physics*, **37**, 725 (1999).
8. S. Dua, R. L. McCullough, and G. R. Palmese, *Polymer Composites*, **20**, 3, 379 (1999).
9. L. T. Drzal and P. J. Herrera-Franco, *Engineered Materials Handbook: Adhesives and Sealants*, **3** (ASM International, Metals Park, Ohio), 391 (1990).
10. J. P. Dunkers, K. M. Flynn, and R. S. Parnas, *Composites Part A*, **28A**, 163 (1997).
11. D. L. Woerdeman, J. K. Spoorer, K. M. Flynn, and R. S. Parnas, *Polymer Composites*, **18**, No. 1, 133 (1997).
12. G. A. Holmes, R. C. Peterson, D. L. Hunston, and W. G. McDonough, *Polymer Composites*, **21**, 3, 450 (2000).
13. C. Schultheisz, C. Schutte, W. McDonough, K. Mac-Turk, M. McAuliffe, S. Kondagunta, and D. Hunston, *ASTM STP 1290*, American Society for Testing and Materials, 103 (1996).
14. J. Whitney and L. Drzal, *ASTM STP 937*, American Society for Testing and Materials, 179, (1997).
15. D. J. Herzog, P. P. Burrell, and M. D. Teigen, 44th Annual Conference, Composites Institute, The Society of the Plastics Industry, 16-C, 1 (1989).

Certain commercial materials and equipment are identified in this study for adequate definition of the experimental procedure. In no instance does such identification imply recommendation or endorsement by the National Institute of Standards and Technology nor does it imply that the materials or instruments are necessarily the best available for this purpose.